ELSEVIER

Thermochimica Acta 343 (2000) 81–88

thermochimica acta

www.elsevier.com/locate/tca

Numerical modeling and analysis of temperature modulated differential scanning calorimetry: On the separability of reversing heat flow from non-reversing heat flow

S.X. Xu[a], Y. Li[a,*], Y.P. Feng[b]

[a]*Departement of Materials Science, Faculty of Science, National University of Singapore, Lower Kent Ridge Road, Singapore*
[b]*Departement of Physics, Faculty of Science, National University of Singapore, Lower Kent Ridge Road, Singapore*

Received 8 June 1999; received in revised form 19 July 1999; accepted 4 August 1999

Abstract

Temperature modulated differential scanning calorimetry (TMDSC) is a recently developed method used to analyze thermal properties of materials such as heat capacity C_p and heat flow under isothermal or continuous heating conditions. However the method of measuring C_p in TMDSC and the separation of reversing heating flow (RHF) from non-reversing heat flow (NHF) depends on the precondition that the system is linear and the effect of non-reversing heat flow is also linear or very close to being so. In this paper, a numerical simulation method is used to study heat capacity C_p, NHF and RHF in various situations. It is found that using Fourier Transform to calculate C_p is applicable under steady state condition where there is no NHF. In the NHF releasing temperature range, the measured C_p value varies with different NHF patterns and modulation conditions even if C_p stays constant over the whole temperature range concerned. It appears that this method should be used with discretion in terms of the explanation of experimental results. Quantitative separation of RHF from NHF still remains a challenge if the mechanism of NHF and its effect on the system is not clear.

Keywords: TMDSC; Numerical simulation; Reversing heat flow; Non-reversing heat flow; Heat capacity

1. Introduction

In the past few years temperature modulated differential scanning calorimetry (TMDSC), a novel method distinct from conventional DSC due to the fact that a sinusoidal heating pattern can be superimposed onto an underlying linear heating rate, has been patented and commercialized [1–3]. However a problem of TMDSC is its reproducibility as has been identified by some works [4,5].

In TMDSC, the temperature of the heating block (T_b) follows the following condition:

$$T_b(t) = T_0 + qt + AT_b\sin(\omega t). \quad (1)$$

Then, correspondingly, the sample and reference temperature will be:

$$T_s(t) = T_0 + qt - \frac{qC_s}{K} + AT_s\sin(\omega t - \varepsilon), \quad (2)$$

$$T_r(t) = T_0 + qt - \frac{qC_r}{K} + AT_r\sin(\omega t - \varphi), \quad (3)$$

where T_0 is the TMDSC system starting temperature, $T_s(t)$ and $T_r(t)$ the sample and reference temperature,

* Corresponding author. Tel.: +65-771-5192; fax: +65-776-3604.
E-mail address: masliy@nus.edu.sg (Y. Li).

0040-6031/00/$ – see front matter
PII: S0040-6031(99)00341-X

respectively, t the time, q the underlying heating rate, C_r and C_s the heat capacities of the reference and sample, respectively, AT_b, AT_r, AT_s the temperature oscillation amplitude of the heating block, reference and sample, respectively, $\omega = 2\pi/p$ the temperature modulation angular frequency, where p the modulation period, ϵ and φ the sample and reference temperature phase angle, and K the system thermal constant, or the inverse of TMDSC system thermal resistance R_d,

$$K = \frac{1}{R_d}. \tag{4}$$

More detailed mathematical descriptions have been given elsewhere [6–9]. Furthermore, if T_0 is constant and the underlying heating rate $q = 0$ or is very small (for example, only a few degrees per min), it has been shown that [6],

$$C_s - C_r = \left(\frac{A\Delta}{AT_s}\right)\sqrt{\left(\frac{K}{\omega}\right)^2 + C_r^2}, \tag{5}$$

where $A\Delta$ is the amplitude of $T_r(t) - T_s(t)$.

In TMDSC, the sample temperature follows the general heat flow equation:

$$\frac{dQ}{dt} = C_p\left(\frac{dT}{dt}\right) + f(T,t), \tag{6}$$

where dQ/dt is the total heat flow, $f(T,t)$ the non-reversing heat flow component that generally depends on both time and temperature, C_p the heat capacity of sample material and dT/dt is the heating rate.

It is possible to measure C_p by deconvolution of the temperature signals based on the assumption that the system is linear or not far from the linear state even with the non-reversing heat flow [6–9], hence the reversing heat flow component $C_p(dT/dt)$ may be separated from the total heat flow.

In this paper, a numerical model is established via ''method of finite differences'' to separate the reversing and non-reversing heat flows. Different types of non-reversing heat flow are adopted to simulate heat flow and temperature changes in TMDSC. A discrete Fourier Transform analysis technique is used to calculate sample heat capacity C_p, total heat flow (HF), reversing heat flow (RHF) and non-reversing heat flow (NHF).

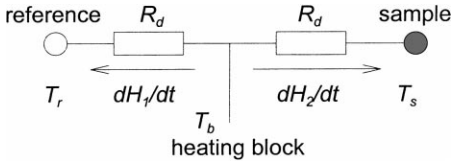

Fig. 1. Simplified TMDSC model. R_d: thermal resistance between heating block and reference or sample (assuming heating block and MDSC cell is symmetric), dH_1/dt, dH_2/dt being the heat flow to reference and sample, respectively.

1.1. Simplified model of TMDSC

Fig. 1 shows a simplified TMDSC model. In this model, heat transfers from the heating block (with a temperature T_b) to both sample and reference. The system is assumed to be symmetric and there is no heat exchange between the sample and reference. The thermal resistance between the heating block and the sample or reference is R_d in each case.

From the above model, one may consider two different heating situations here:

(a) When there is no non-reversing heat flow involved, according to Newton's law of heat conduction:

$$\frac{dH_1}{dt} = \frac{(T_b - T_r)}{R_d} = C_r\frac{dT_r}{dt}. \tag{7}$$

Here $C_r = c_{p\_r}M_r$, where c_{p_r} is the specific heat capacity of reference, M_r the reference pan mass, and

$$\frac{dH_2}{dt} = \frac{(T_b - T_s)}{R_d} = C_s\frac{dT_s}{dt}, \tag{8}$$

where $C_s = c_{p\_r}M_r + c_{p\_s}M_s$, C_s is the total heat capacity of sample and sealing pan, c_{p_s} the sample specific heat capacity, and M_s is the sample mass (the sample is sealed in the same pan as reference pan).

By subtracting Eq. (7) from Eq. (8), we can obtain:

$$\frac{dH_2 - dH_1}{dt} = \frac{(T_r - T_s)}{R_d} = K(T_r - T_s), \tag{9}$$

where $(dH_2 - dH_1)/dt$ is the heat flow to heat the sample less than the sealing pan in the TMDSC instrument. K is a TMDSC system constant that can be calibrated by testing materials with well known thermal properties such as indium or sapphire.

(b) If there is non-reversing heat flow NHF(T,t) during the heating or cooling process, then Eq. (8) becomes:

$$\frac{dH_2}{dt} + \mathrm{NHF}(T,t) = \frac{(T_b - T_s)}{R_d} + \mathrm{NHF}(T,t) = C_s \frac{dT_s}{dt}. \quad (10)$$

With Eqs. (7)–(10), the following differential equations can be obtained with Finite Differences Method (as the basis for further simulations) under the condition of heating or cooling without NHF:

$$dT_r = \frac{dH_1}{C_r} = \frac{T_b - T_r}{R_d C_r} dt, \quad (11)$$

$$dT_s = \frac{dH_2}{C_s} = \frac{T_b - T_s}{R_d C_s} dt, \quad (12)$$

and under the condition of heating (or cooling) with NHF:

$$dT_r = \frac{dH_1}{C_r} = \frac{T_b - T_r}{R_d C_r} dt, \quad (13)$$

$$dT_s = \frac{dH_2 + \mathrm{NHF}(T,t)dt}{C_s} = \left(\frac{T_b - T_s}{R_d} + \mathrm{NHF}(T,t)\right)\left(\frac{dt}{C_s}\right). \quad (14)$$

1.2. Heating simulation and data treatment:

The purpose of this simulation is to find out how "measured" C_p, HF, RHF and NHF values will differ from given values and the separability of RHF from NHF, which consists of the following steps:

1. Let the heating block temperature follow a given modulated heating curve.
2. At a certain time or temperature, a non-reversing heat flow is "triggered" artificially and varies according to the NHF release patterns.
3. Calculate the temperatures of sample, reference and heating block, $T_b(t)$, $T_r(t)$, $T_s(t)$, and heat flow to the sample and reference, $dH_1(t)/dt$, $dH_2(t)/dt$.
4. Use a discrete Fourier Transform (with a sliding transform window) to find the first order harmonics and underlying part of $(T_r - T_s)$ and T_s so as to calculate sample specific heat capacity c_{p_s} and HF(t).
5. With the sample specific heat capacity c_{p_s} and HF, it is simple to obtain the reversing heat flow:

$$\mathrm{RHF}(t) = c_{p\_s} M_s \left(\frac{dT_s}{dt}\right), \quad (15)$$

and non-reversing heat flow:

$$\mathrm{NHF}(t) = \mathrm{HF}(t) - \mathrm{RHF}(t). \quad (16)$$

To simulate actual modulation heating experiments, the temperature of the heating block assumes the form of Eq. (1). Because this is an idealized model, it is reasonable to assume that irrespective of the underlying heating rate, modulation amplitude, modulation frequency and initial temperatures, the temperature gradient inside the sample and reference pans is always negligible. Also we assume that the heat capacity C_p of the test sample remains constant over the whole temperature range concerned.

In the following simulation, two arbitrary NHF patterns are adopted: a temperature dependent NHF pattern and a time dependent NHF pattern. There is an important difference between the above two NHF patterns. For time dependent NHF, once the non-reversing heat flow process begins, it only varies with time but not with temperature, hence its intensity cannot be modulated by the sinusoidal part of heating block temperature. In other words, it is not sensitive to minor temperature variations, while for the temperature dependent NHF, it will be modulated by the heating pattern.

In the simulation, the non-reversing reaction follows the energy distribution function (with a single variable):

$$\int_{X1}^{X2} H(X)dX = C. \quad (17)$$

Here, the non-reversing reaction will only occur between parameter range $X1$ and $X2$ (either time or temperature range). C is the total NHF energy. $H(X) = 0$ for the region outside $X1$ to $X2$. To facilitate numerical analysis, let

$$H(X) = \frac{2SC\sin^2[S(X - X_0)]}{\pi}. \quad (18)$$

It is easy to prove that $H(X)$ satisfies the following with the above assumption:

$$\int_{X_0}^{X_0 + \pi/S} \frac{2SC\sin^2[S(X - X_0)]}{\pi} dX = C, \quad (19)$$

Table 1
Numerical simulation parameters

Parameter	Description	Value
C_{p_r}	Specific heat capacity of reference pan (J/g K)	0.951
C_{p_s}	Specific heat capacity of sample (J/g K)	0.134
M_r	Reference and sample pan mass (mg)	24
M_s	Sample mass (mg)	20
R_d	System thermal resistance (°C/W)	108
dt	Time step for finite differences method(s)	0.0001
C	NHF total energy (J/g)	6
A	Modulation amplitude (°C)	0.20
q	Underlying heating rate (°C/min)	3
p	TMDSC modulation period(s)	30

where X_0 is the NHF start time or temperature, $X_0 + \pi/S$ the NHF end time or temperature, and S is the NHF occurrence time or temperature range adjusting factor. Because the total non-reversing reaction energy is fixed by C, by varying S, the range can be increased thus to lower the NHF peak intensity, or the range can be decreased in order to increase the NHF peak intensity. Computer simulation parameters are listed in Table 1. The values selected are typical of those used in actual TMDSC experiments. The system thermal resistance is obtained by comparing the heat flow, reference and sample temperature difference signals in a TA Instruments DSC 2920 heating curve.

2. Results and analysis

2.1. Temperature dependent NHF

Figs. 2 and 3 are the TMDSC simulation results for the temperature dependent NHF release curve as discussed above. In Fig. 2, the NHF release temperature range is preset from 200°C to 250°C. There are more than 10 modulation cycles during the NHF

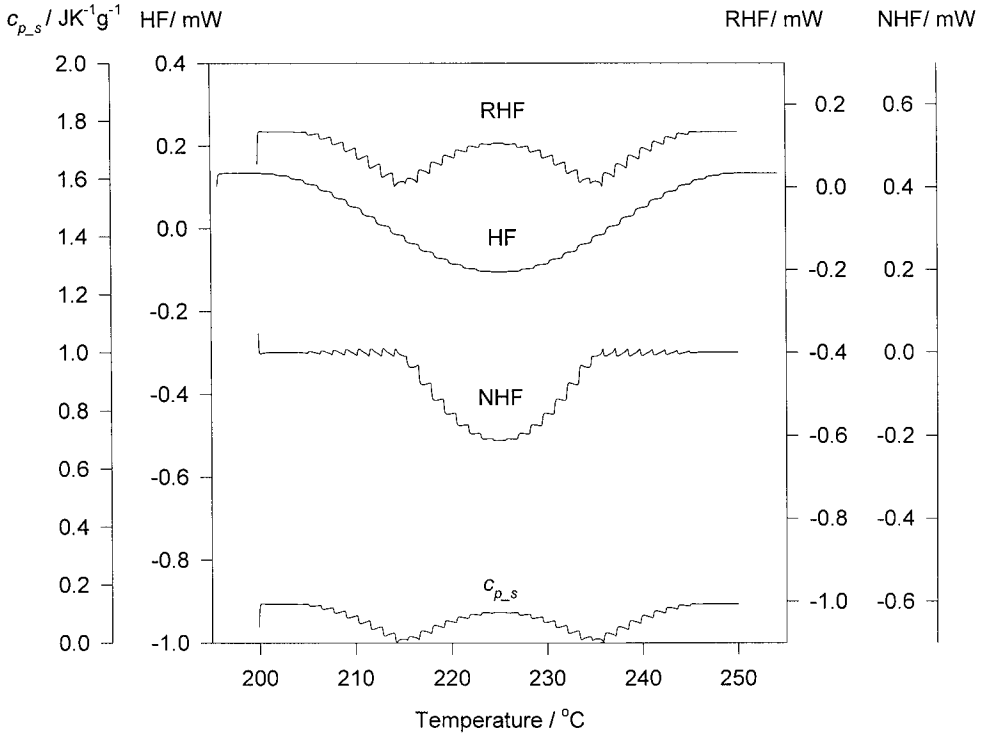

Fig. 2. Deconvoluted c_{p_s}, HF, RHF and NHF when NHF is temperature dependent, with more than 10 modulation cycles in the NHF release process.

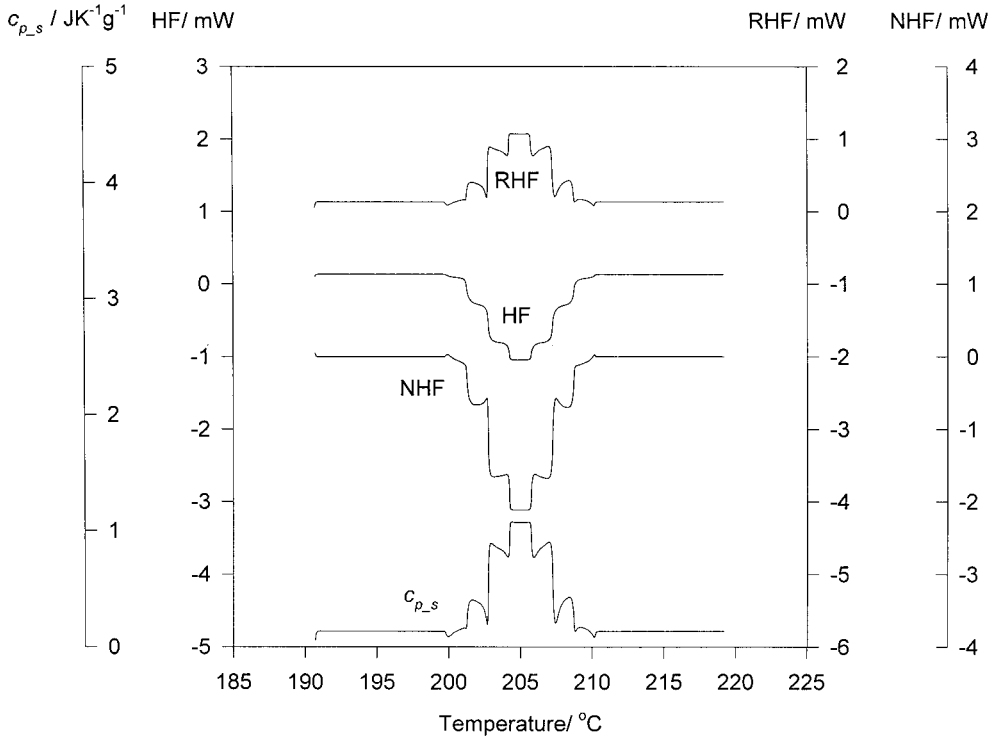

Fig. 3. Deconvoluted c_{p_s}, HF, RHF and NHF when NHF is temperature dependent, with only five modulation cycles in the NHF release process.

process in this simulation. Due to its larger NHF release range, the NHF peak intensity is thus lower than that in Fig. 3 (the total NHF energy is the same in both cases), but it takes a longer time to complete NHF release, hence representing a "slow" process. In Fig. 3, the NHF release range is preset from 200°C to 210°C, there are only five modulation cycles within this region. Compared to Fig. 2, this represents a relatively faster NHF release process.

As can be clearly seen, sample specific heat capacity c_{p_s} at steady state where there is no NHF can be accurately deconvoluted from the simulation data. When the temperature dependent NHF begins, although HF curves are similar in the two simulations (the only differences are the duration and peak values), the c_{p_s} value obtained by discrete Fourier Transform varies drastically from Fig. 2 to Fig. 3. As do the reversing heat flow and non-reversing heat flow. The original material c_{p_s} can no longer be recovered during the NHF incidence. In Fig. 2, two "valleys" show up in the C_p curve with a "hump" between the two while in Fig. 3, a strong peak appears in the c_{p_s} curve, with a maximum far greater than the given value under steady state.

2.2. Time dependent NHF

Figs. 4 and 5 are the simulation results for time dependent NHF release process. The only difference between the two is the NHF process time range. The deconvoluted sample c_{p_s} value at steady state both before and after the NHF process still remains the same as the given simulation value (0.134 J/kg). This helps to explain why in TMDSC the materials heat capacity C_p could be effectively measured in a single run with the precondition that no non-reversing heat flow is involved.

From Figs. 4 and 5, it is found that if there are more modulation cycles in the NHF reaction, the deconvoluted c_{p_s} has much smaller deviation from the true

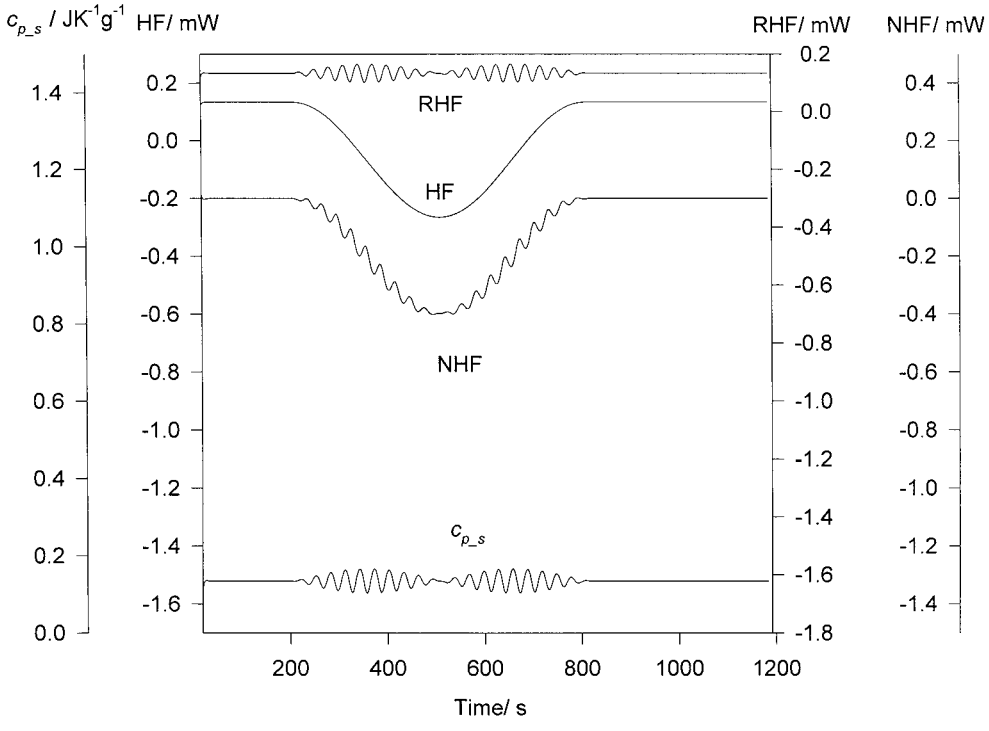

Fig. 4. Deconvoluted c_{p_s}, HF, RHF and NHF when NHF is time dependent, with more than 10 modulation cycles in the NHF release process.

value of c_{p_s}. With further data smoothing treatment, the "measured" c_{p_s} will be fairly close to the accurate value even if there is such a non-reversing heat flow occurring as illustrated in Fig. 4.

Lacey et al. [10] reported their analytical solutions, in which the NHF is a first-order chemical reaction that is both time and temperature dependent. With a number of approximations in the analysis, their results also show that the "measured" heat capacities of the sample exhibit deviations during the endothermic reaction where it had been assumed that the heat capacity stays constant, and the peak values can be decreased by increasing the modulation frequency. Another factor that can affect the result is how sensitive the NHF reaction to temperature changes. These are consistent with our present simulation results. For certain kinds of reactions that take a relatively longer time to complete, this approach may be feasible to obtain a better result, while for other NHF reactions that are complete in a much shorter time or in a very narrow temperature range, then it has some limitations. The instrument thermal inertia and resolution set a lower limit to the modulation period (for example, TA Instruments DSC2920's suggested minimum modulation period is 10 s), temperature gradients inside the sample will also increase with increased frequencies. These factors could contribute to test errors and complicate experimental result interpretation. Besides, according to the numerical simulations as shown in Figs. 2 and 3, it seems even if there is no limitations to the modulation frequency, whether the measured (actually deconvoluted) heat capacities truly reflect materials heat capacities still depends on the characteristics of the reaction itself, that is, its time and temperature dependency.

The Fourier Transform is applicable to linear thermal response systems [11,12]. Should satisfactory results be obtained, the whole system (including the measurement instrument and sample parameters to be tested) should meet the superimposition principle.

In a real situation, NHF may occur in the form of chemical reactions, kinetic events such as crystalliza-

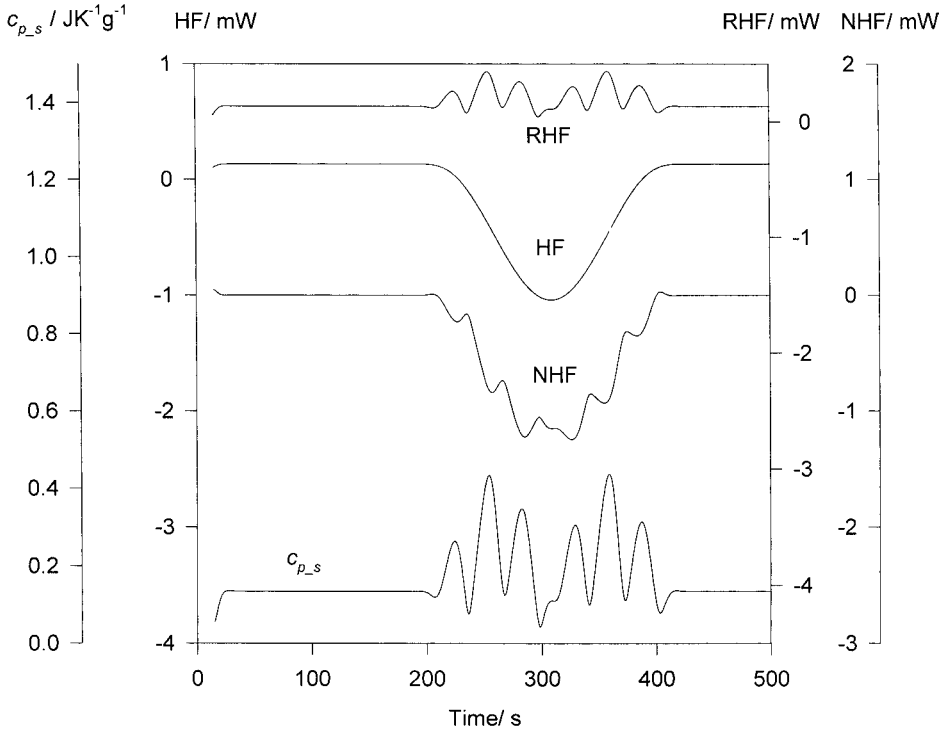

Fig. 5. Deconvoluted c_{p_s}, HF, RHF and NHF when NHF is time dependent, with only six modulation cycles in the NHF release process.

tion from amorphous state, recrystallization or a complex combination of some of them. The resultant NHF pattern could be much more complicated than those used in the model. Furthermore the heat capacity of the sample may actually change during the reaction depending on the nature of NHF release process, thus the system could be far from linear. In this case, although qualitative separation of reversing and non-reversing one is possible, quantitative separation still remains to be solved.

3. Conclusions

From the above simulations, the heat capacity of the sample seems to be heavily dependent on the NHF pattern and the modulation conditions. The measurement of C_p is quite applicable for steady state where there is no NHF. If NHF is only time dependent and the modulation frequency is high enough, it is still possible to allow relatively good deconvolution of C_p, HF, RHF and NHF. When NHF is strongly temperature dependent, its effect on the heating process is nonlinear and could influence the thermodynamic responses to such an extent that the deconvoluted results can no longer accurately reflect materials true heat capacities. With both C_p and $f(T,t)$ unknown in the general heat conduction Eq. (6) when there is a non-reversing heat flow incidence, care must be taken when explaining the deconvoluted C_p, HF, RHF and NHF.

References

[1] M. Reading, D. Elliott, V.L. Hill, J. Therm. Anal. 40 (1993) 949–955.
[2] P.S. Gill, S.R. Sauerbrunn, M. Reading, J. Therm. Anal. 40 (1993) 931–939.
[3] Reading et al., US Patent No. 5,224,775 (6 July 1993).
[4] J.E.K. Schawe, Thermochim. Acta 271 (1996) 127–140.
[5] J.E.K. Schawe, G.W.H. Höhne, J. Therm. Anal. 46 (1996) 893–903.

[6] B. Wunderlich, Y. Jin, A. Boller, Thermochim. Acta 238 (1994) 277.
[7] A. Boller, Y. Jin, B. Wunderlich, J. Therm. Anal. 42 (1994) 307–330.
[8] M. Varma-Nair, B. Wunderlich, J. Therm. Anal. 46 (1996) 879–892.
[9] B. Wunderlich, J. Therm. Anal. 48 (1997) 207–224.
[10] A.A. Lacey, C. Nikolopoulos, M. Reading, J. Therm. Anal. 50 (1997) 279–333.
[11] T. Ozawa, K. Kanari, Thermochim. Acta 288 (1996) 39–51.
[12] B. Wunderlich, A. Boller, I. Okazak, S. Kreitmeier, Thermochim. Acta 282/283 (1996) 143–155.